Year: 2012

The proton-activated G protein coupled receptor OGR1 acutely regulates the activity of epithelial proton transport proteins

Mohebbi, Nilufar; Benabbas, Chahira; Vidal, Solange; Daryadel, Arezoo; Bourgeois, Soline; Velic, Ana; Ludwig, Marie-Gabrielle; Seuwen, Klaus; Wagner, Carsten A

Abstract: The Ovarian cancer G protein-coupled Receptor 1 (OGR1; GPR68) is proton-sensitive in the pH range of 6.8 - 7.8. However, its physiological function is not defined to date. OGR1 signals via inositol trisphosphate and intracellular calcium, albeit downstream events are unclear. To elucidate OGR1 function further, we transfected HEK293 cells with active OGR1 receptor or a mutant lacking 5 histidine residues (H5Phe-OGR1). An acute switch of extracellular pH from 8 to 7.1 (10 nmol/l vs 90 nmol/l protons) stimulated NHE and H(+)-ATPase activity in OGR1-transfected cells, but not in H5Phe-OGR1-transfected cells. ZnCl(2) and CuCl(2) that both inhibit OGR1 reduced the stimulatory effect. The activity was blocked by chelerythrine, whereas the ERK1/2 inhibitor PD 098059 had no inhibitory effect. OGR1 activation increased intracellular calcium in transfected HEK293 cells. We next isolated proximal tubules from kidneys of wild-type and OGR1-deficient mice and measured the effect of extracellular pH on NHE activity in vitro. Deletion of OGR1 affected the pH-dependent proton extrusion, however, in the opposite direction as expected from cell culture experiments. Upregulated expression of the pH-sensitive kinase Pyk2 in OGR1 KO mouse proximal tubule cells may compensate for the loss of OGR1. Thus, we present the first evidence that OGR1 modulates the activity of two major plasma membrane proton transport systems. OGR1 may be involved in the regulation of plasma membrane transport proteins and intra- and/or extracellular pH.

DOI: 10.1159/000338486

Original Paper

Cellular Physiology and Biochemistry

Cell Physiol Biochem 2012;29:313-324

Accepted: February 28, 2012

The Proton-activated G Protein Coupled Receptor OGR1 Acutely Regulates the Activity of Epithelial Proton Transport Proteins

Nilufar Mohebbi[1], Chahira Benabbas[1], Solange Vidal[2], Arezoo Daryadel[1], Soline Bourgeois[1], Ana Velic[1], Marie-Gabrielle Ludwig[2], Klaus Seuwen[2] and Carsten A. Wagner[1]

[1]Institute of Physiology and Zurich Center for Integrative Human Physiology (ZIHP), University of Zurich, Zurich, [2]Novartis Institutes for BioMedical Research, Novartis Pharma AG, Basel

Key Words

Acid sensing • NHE exchanger • H-ATPase • Kidney • Proximal tubule

Abstract

The Ovarian cancer G protein-coupled Receptor 1 (OGR1; GPR68) is proton-sensitive in the pH range of 6.8 - 7.8. However, its physiological function is not defined to date. OGR1 signals via inositol trisphosphate and intracellular calcium, albeit downstream events are unclear. To elucidate OGR1 function further, we transfected HEK293 cells with active OGR1 receptor or a mutant lacking 5 histidine residues (H5Phe-OGR1). An acute switch of extracellular pH from 8 to 7.1 (10 nmol/l vs 90 nmol/l protons) stimulated NHE and H^+-ATPase activity in OGR1-transfected cells, but not in H5Phe-OGR1-transfected cells. $ZnCl_2$ and $CuCl_2$ that both inhibit OGR1 reduced the stimulatory effect. The activity was blocked by chelerythrine, whereas the ERK1/2 inhibitor PD 098059 had no inhibitory effect. OGR1 activation increased intracellular calcium in transfected HEK293 cells. We next isolated proximal tubules from kidneys of wild-type and OGR1-deficient mice and measured the effect of extracellular pH on NHE activity *in vitro*. Deletion of OGR1 affected the pH-dependent proton extrusion, however, in the opposite direction as expected from cell culture experiments. Upregulated expression of the pH-sensitive kinase Pyk2 in OGR1 KO mouse proximal tubule cells may compensate for the loss of OGR1. Thus, we present the first evidence that OGR1 modulates the activity of two major plasma membrane proton transport systems. OGR1 may be involved in the regulation of plasma membrane transport proteins and intra- and/or extracellular pH.

Introduction

Protons are produced by metabolism and are excreted from cells by various pathways [1-3]. However, protons can also function as signals. For instance in *C. elegans*, protons may act as neurotransmitters and induce contraction of certain muscles [4, 5]. The mechanism involves two genes encoding cation channels, pbo-5 and pbo-6, which are part of the proton sensing and signaling complex [4]. Mammals possess several proton-activated channels or receptors, including the proton-activated ASIC

KARGER

Fax +41 61 306 12 34
E-Mail karger@karger.ch
www.karger.com

1015-8987/12/0294-0313$38.00/0

Accessible online at:
www.karger.com/cpb

Carsten A. Wagner
Institute of Physiology and Zurich Center for Integrative Human Physiology (ZIHP), University of Zurich, Winterthurerstrasse 190, CH-8057 Zurich (Switzerland)
Tel. +41-44-63 55023, Fax +41-44-63 56814, E-Mail Wagnerca@access.uzh.ch

channels [6], proton-sensitive TRP channels [7], and the calcium-sensing receptor [8-10]. However, these receptors or channels are activated or modulated by high proton concentrations (pH 5-6.5) occurring in specialized compartments. Nonetheless, proton concentrations in the physiologic range (pH 7.2-7.4) can activate a recently identified G protein-coupled receptor subfamily [11, 12]. This subfamily comprises three members: ovarian cancer G protein-coupled receptor 1 (OGR1; GPR68), G protein-coupled receptor 4 (GPR4), and T cell death-associated gene 8 (TDAG8; GPR65) [11, 12]. Ludwig et al. showed that OGR1 acts as a proton-activated receptor, which stimulates inositol trisphosphate (IP_3) formation, thereby releasing intracellular calcium, and activates the mitogen-activated protein kinase/extracellular signal-regulated (ERK) kinase cascade. However, the downstream OGR1 targets are elusive and little is known about their physiological role [11, 12]. Eliminating OGR1 in mice shed little light on the problem, since no clear-cut phenotype was reported [13]. We focused our attention on OGR1 and found that the receptor regulates NHE3 and H^+-ATPase, in response to extracellular pH changes in cultured renal cells. This activation requires a cluster of histidine residues in the extracellular domains of the receptor and protein-kinase C (PKC) activation. Additionally, we studied wild-type and OGR1-deficient mice and found that OGR1 modulates the pH-sensitive response of NHE3 in isolated proximal tubules.

Materials and Methods

OGR1 knockout mice

Ogr1 deficient mice were generated by and obtained from Deltagen, Inc. - San Mateo, Ca, USA. The OGR1 targeting vector was constructed using a 4 kb fragment of mouse genomic DNA in which 501 bp of the coding sequence (ATG TGA CCG TGC TGG TGG TG … ACC GCT TCC TGG TGG GCT TT) were replaced by a LacZ-Neo cassette. The targeting vector, containing 1.9 kb of 5' flanking (the left arm) and 2.1 kb of 3' flanking (the right arm) sequence homology, was electroporated into 129/OlaHsd ES cells. Genomic DNA from the recombinant ES line was assayed for homologous recombination by PCR, using a gene-specific (for the 5' end: TGT TGG GGT GGA GGA CAA GAC TTG G; for the 3' end: GCA ACC CCC ATC TTG CCC TTG GAT C) primer, which lies outside of and adjacent to the targeting vector arm, paired in succession with one of three Neo primers in the insertion fragment. The targeted allele was further confirmed at the 5'end by Southern blot analysis: genomic DNA isolated from ES lines was digested with EcoRI or EcoRV (determined to cut outside of the construct arms) and probed with a radiolabeled DNA fragment that hybridizes outside of and adjacent to the construct arm. Targeted ES cells were injected into blastocysts harvested from C57BL/6 mice. The resulting chimeric males were crossed with C57BL/6 females for selection of F1 mice with germ line transmission of the targeted OGR1 allele. F2 homozygous mutant mice were produced by intercrossing F1 heterozygous males and females. Genotyping was performed by PCR on genomic DNA, using following primers:

P1 – CCA GCA GCA GGC AGA TGG GGA AGA G, on the 3'arm of the targeting vector

P2 – GGG TGG GAT TAG ATA AAT GCC TGC TCT, on the Neo sequence

P3 – CTT CCA CCA GTT CCG GAC CCT GAA G, on the 5' arm of the targeting vector

PCR product sizes are 424 bp for the targeted allele (P1-P2) and 223 bp for the endogenous allele (P1-P3).

F1 mice were backcrossed to C57BL/6 for at least 6 generations before performing phenotyping studies. Animals were housed under standard conditions with free access to food and water. *Ogr1*$^{-/-}$ mice were born at the expected Mendelian ratio, showed no obvious gross anatomical abnormalities, postnatal survival, growth, body weight, and fertility were undistinguishable from wild type and heterozygous litters. Histological analysis of various tissues including kidney did not show any abnormalities (data not shown). The use of mice was according to Swiss Animal Welfare Laws, corresponding to APS guidelines, and approved by the local veterinary authority (Kantonales Veterinäramt Zürich, CH).

Tubular isolation, cell culture and preparation

Proximal tubules were isolated from wild type or *Ogr1*$^{-/-}$ mouse kidneys and transferred onto glass coverslips as described previously [14, 15]. HEK293 cells and HEK293 cells stably transfected either with the human wild type OGR1 construct or an OGR1 mutant lacking 5 histidine residues placed on top of helices I, IV and VII, and in extracellular loops 1 and 2 (H17, H20, H84, H169 and H269, substituted by phenylalanine: H5Phe) were described previously [11]. All cells were maintained in Dulbecco's modified Eagle's medium/Ham's F-12 medium (Gibco, Switzerland) (1:1) supplemented with 10% fetal calf serum (Amimed, Switzerland) in a humidified atmosphere of 5% CO_2, 95% air at 37°C. Stable cell populations expressing the OGR1 receptor were isolated following selection with antibiotic G418 (400 µg/ ml). For all pH experiments, cells were passaged, disseminated onto coverslips and grown to subconfluency for 48 hours. The final medium exchange was performed 24 hours before the experiments were started. Medium pH was maintained at pH 7.4.

Intracellular pH and Ca^{2+} measurements

For pH_i measurements, either individual slides coated with cells or coverslips precoated with the cell adhesive Cell-Tak (BD Biosciences, Bedford, MA, USA) containing selected tubules were transferred to a perfusion chamber (~ 3-5 ml/min flow rate). The temperature of the chamber was maintained at 37°C by an electronic feedback circuit. The control bath solution was initially a HEPES-buffered Ringer solution (125 mM NaCl/ 5 mM KCl/ 1 mM $CaCl_2$/ 1.2 mM $MgSO_4$/ 2 mM NaH_2PO_4/ 32.2 mM HEPES/ 5 mM Glucose). Cell coated slides or single tubule

fragments were loaded with the acetoxymethyl ester of the pH-sensitive dye BCECF (10 µM, Molecular Probes, Oregon, USA) for 10 min and washed to remove all non-deesterified dye. Loading of cells and tubule fragments was performed in control solution at pH 8 to reduce OGR1 receptor activity.

pH_i was measured microfluorometrically by exciting the dye with a spot of light alternately at 490 and 440 nm while monitoring the emission at 532 nm with a video-imaging system [14, 16]. Intracellular acidification was induced using the NH_4Cl (20 mM) prepulse technique for 5 min and then washed into a Na^+-free solution [17]. To measure H^+-ATPase activity, bicarbonate-free solutions were used and Na^+ was replaced by N-methyl-D-glucamine (NMDG). Sodium-proton-exchanger (NHE) activity was calculated from the slope of the initial rapid intracellular alkalinization after re-addition of Na^+. Each experiment was calibrated for pH_i using the nigericin/high K^+ method [18] and the obtained ratios were converted to pH_i. Na^+-independent pH_i recovery rates in response to an acid load were calculated in non-transfected and stably transfected cells with OGR1 or the OGR1 mutant H5Phe as well as in proximal tubules from wild type and *Ogr1*$^{-/-}$ mice. Na^+-dependent pH_i recovery was measured in proximal tubules in the pH_i range of 6.55–6.85. The pH_i range chosen represented the average values found in the respective tubule segment. Data are shown as changes in pH_i (ΔpH_i) per minute.

For intracellular calcium measurements, cells were seeded at 10000 cells/well in 384-well black clear bottom plates (Greiner, Switzerland). After overnight growth, cell culture medium was removed and 20 µl of the loading buffer was added for 1 hour (HBSS1X/HEPES 20mM, pH7.9) containing the calcium-sensitive fluorescent dye calcium 5 and probenecid (Sigma, Buchs, Switzerland) at 2.5 mM. After 1 hour incubation at 37°C, intracellular calcium was measured by increases in fluorescence over time using the FDSS7000 (Hamamatsu, Solothurn, Switzerland) after stimulation of the cells by addition of an appropriate amount of acidic buffer to reach the required pH. Two fluorescence values were exported: F_{basal} corresponding to the average of the baseline value before buffer injection and F_{max}, the maximum fluorescence during the reading time. The calcium response was then normalized to the calcium baseline values according to the formula $dF/F = (F_{max} - F_{basal}) / F_{basal}$.

In a second set of experiments, calcium was measured using video-imaging on the same setup as used for intracellular pH measurements. For Ca^{2+} measurements in cells, individual cell-coated slides were transferred to a perfusion chamber (≈3-5 ml/min flow rate). The temperature of the chamber was maintained at 37°C by an electronic feedback circuit. The control solution was initially a HEPES-buffered Ringer solution (130.7 mM NaCl, 5 mM KCl, 2 mM NaH_2PO_4, 1.2 mM $MgSO_4$, 10.5 mM Glucose, 2 mM Glutamine, 1 mM $CaCl_2$, 32.5 mM HEPES, pH 8). Cell coated slides or single tubule fragments were loaded with the Ca^{2+}-sensitive dye FURA-2 (10 µg/ml, Molecular Probes, Oregon, USA) for 20 min and then washed. Ca^{2+} measurements on mouse nephron segments were performed on hand dissected proximal tubules and outer medullary collecting ducts. In brief, mice were anesthetized with intraperitoneal injections of xylazine/ketamine. Both kidneys were cooled in situ with ice-cold control solution for one minute and then removed and cut into thin coronal slices for tubule dissection. Proximal straight tubules (S3 segments) and outer medullary collecting ducts (OMCDs) were dissected, respectively, from the cortex medullary rays and the medulla at 4°C in control solution and the isolated nephron segment was transferred to the bath chamber.

To measure intracellular calcium FURA-2 was excited with light of 340/380 nm wavelengths. After loading with FURA-2 cells or nephron segments were first superfused with control solution at pH 8 and subsequently with control solution at pH 6.8. ATP at a concentration of 1 mM was used as control before starting the calibration using ionomycin at a final concentration of 1 µM. $[Ca^{2+}]_i$ was calculated from the ratio of fluorescence at excitations of 340/380 nm using the following equation as described previously: $Ca_i^{2+} = [(R - Rmin)/(Rmax - R)] \times (Fmin/Fmax) \times Kd$, where R is the measured ratio of emitted light, Rmin, Rmax and Fmax are the fluorescence values at 380 nm with 1 mM Ca^{2+} bath solution, Fmin is the fluorescence at 380 nm with 0 mM Ca^{2+} bath solution, and the dissociation constant (Kd) = 225 nM for Fura-2-calcium binding [19].

Chemicals were added to the perfusion solutions from stock solutions at the given concentrations for each experimental protocol. All chemicals were of highest purity and were purchased from Sigma (Buchs, Switzerland) if not annotated otherwise.

HEK cell lysate preparation (membrane fraction) and immunoblotting

Cultures of HEK293 and OGR1-transfected cells were grown to confluency and washed 2x with PBS. Cells were lysed in a resuspension buffer (200 mM Mannitol, 80 mM HEPES, 41 mM KOH, pH 7.5) and protease inhibitor mixture (1:1000, Roche Diagnostics, Indianapolis, IN, USA) by sonication, and centrifuged at 3000 rpm at 4°C for 10min. The supernatant was removed for a subsequent ultracentrifugation step at 41000 rpm at 4°C for 1 hour. The resulting pellets were resuspended in 200– 300 µl resuspension buffer and the protein concentrations were determined (BioRad Dc Protein Assay, Bio-Rad, Hercules, CA, USA). 75 µg of crude membrane protein was solubilized in Laemmli sample buffer, and SDS-PAGE was performed on 10% polyacrylamide gels. Proteins were transferred electrophoretically from gel to a polyvinylidene difluoride membrane (Immobilon-P, Millipore, MA, USA). After blocking with 5% milk powder in Tris-buffered saline containing 0.1% Tween 20 for 60 min, the blots were incubated with the mouse monoclonal anti-c-myc primary antibody (Invitrogen, Oregon, USA) at the dilution of 1:5000 overnight at 4°C. After washing and subsequent blocking, blots were incubated with the secondary antibody (anti-mouse Ig, horseradish peroxidase conjugated, GE Healthcare UK limited, United Kingdom) at the dilution of 1:10000 for 1 h at room temperature. Antibody binding was detected with the Immobilon Western Chemiluminescent horse radish peroxidase substrate (Millipore, Billerica, MA, USA), using the DIANA III-chemiluminescence detection system (Raytest, Germany). All images were analyzed using appropriate software (Advanced Image Data Analyzer, Raytest, Germany).

	Primer	Fw Rv	Probe	Amplicon length
Pyk-2	5' CAC AAT GCA CTG GAC AAA AAG T 3' 5' CTG CAT CTG CTT TGG GAA A 3'		5' CCT GGA AAA AGA AGT CGG TCT GGA CC3'	84
GPR4	5' CCT GGG CAC TCA TGT TGC T 3' 5' GGT GGA CAC ACT GCT CTG CA 3'		5' TGC TAC CGT GGC ATC CTG AGG GC 3'	84
HPRT	5' TTA TCA GAC TGA AGA GCT ACT GTA ATG ATC 3' 5' TTA CCA GTG TCA ATT ATA TCT TCA ACA ATC 3'		5' TGA GAG ATC ATC TCC ACC AAT AAC TTT TAT GTC CC 3'	127

Table 1. Primers and probes used for quantitative real-time RT-PCR

IP formation assay (radiometric assay)

Confluent cell cultures grown in 24-well plates were labeled with myo[^{3}H]inositol (100 MBq/ml; ART/Anawa Trading, Wangen-Duebendorf, Switzerland) for 24h in serum-free DMEM medium. Cells were then incubated at 37°C in HEPES buffer (HBS: 130 mM NaCl, 0.9 mM NaH_2PO_4, 5.4 mM KCl, 0.8 mM $MgSO_4$, 1.0 mM $CaCl_2$, 25 mM glucose, 20 mM HEPES). The pH of all solutions was adjusted to the indicated value at room temperature. Lithium (20 mM) was added as indicated to block inositol monophosphatase activity, leading to accumulation of IP1 [20-22]. Incubation time was 20 minutes. Cells were then extracted with ice-cold formic acid and total IPs separated from free inositol using batch column chromatography exactly as described before [23].

Preparation of isolated proximal tubule segments for RNA extraction

Male C57Bl/6 mice were anesthetized and perfused through the left ventricle with a HBSS (Hank's Balanced Salt Solution 1x, Gibco) solution containing 1 mg/ml collagenase type IA (Sigma C9891). Kidneys were immediately removed, and after further removal of the capsule thin coronal slices containing both cortex and medulla were prepared and the inner medulla resected. Tissue was incubated at 37°C for approximately 15 min. The digestion was stopped by washing with an ice-cold solution, then the supernatant was removed carefully and twicely washed with 10 ml ice-cold HBSS to remove collagenase. Dissection was performed under a stereo microscope at 4°C using two fine forceps (Dumont no.5). Approximately fifty S3 segments were collected and placed in 300 µl RLT-Buffer (Qiagen, Basel, Switzerland) containing 3 µl 2-mercaptoethanol. Segments were dissected from five different mice. Collected tissue was immediately frozen at –80°C until further RNA extraction.

RNA extraction and quantitative real-time RT-PCR from microdissected nephron segments

Total RNA was extracted using the RNeasy Micro Kit (Qiagen, Basel, Switzerland) according to the manufacturer's instructions. Quality and concentration of the isolated RNA preparations were analyzed using the ND-1000 spectrophotometer (NanoDrop Technologies, DE, USA).

To generate complementary DNA (cDNA), each RNA sample was diluted to 10 ng/µl and was used as a template for reverse transcription using the TaqMan Reverse Transcription Kit (Applied Biosystems, Forster City, CA). Quantitative real-time (qRT-PCR) was performed on the ABI PRISM 7700 Sequence Detection System (Applied Biosystems). Primers for all genes of interest were designed using Primer3 Software (Table 1). For TDAG8 (GPR65) we used the pre-developed TaqMan reagent (Mm00433695_m1) (Applied Biosystems, Darmstadt, Germany). Probes were labeled with the reporter dye FAM at the 5' end and the quencher dye TAMRA at the 3' end (Microsynth, Balgach, Switzerland). The specificity of all primers was first tested in a standard PCR and always resulted in a single product of the expected size on 2% agarose gels (data not shown). Real-time PCR reactions were performed using the TaqMan Universal PCR Master Mix (Applied Biosystems). Briefly 3 µl cDNA, 0.8 µl of each primer (25 µM), 0.4 µl labeled probe (5 µM), 5.2 µl RNase-free water, 10 µl TaqMan Universal PCR Master Mix reached 20.2 µl of final reaction volume. Reaction conditions were: denaturation at 95°C for 10 min followed by 50 cycles of denaturation at 95°C for 15 s and annealing/elongation at 60°C for 60 s with autoramp time. All reactions were run in duplicate. To analyze the data, we set the threshold to 0.06 as this value had been determined to be in the linear range of the amplification curves for all mRNAs in all experimental runs. The expression of gene of interest was calculated in relation to hypoxanthine guanine phosphoribosyl transferase (HPRT). Relative expression ratios were calculated as $R = 2^{[Ct(HPRT)–Ct(test\ gene)]}$, where Ct represents the cycle number at the threshold 0.06.

Statistical analysis

All data are presented as means ± SEM. All data were tested for significance using the unpaired t-Test or one way ANOVA test, and only results with $p < 0.05$ were considered statistically significant.

Results

Activation of OGR1 stimulates NHE and H^+-ATPase activity

We established several clones of HEK293 cells stably expressing OGR1, which also endogenously express various transport proteins involved in renal acid secretion such as the sodium/proton exchanger NHE3 or V-type H^+-ATPases [24]. Since we did not observe any

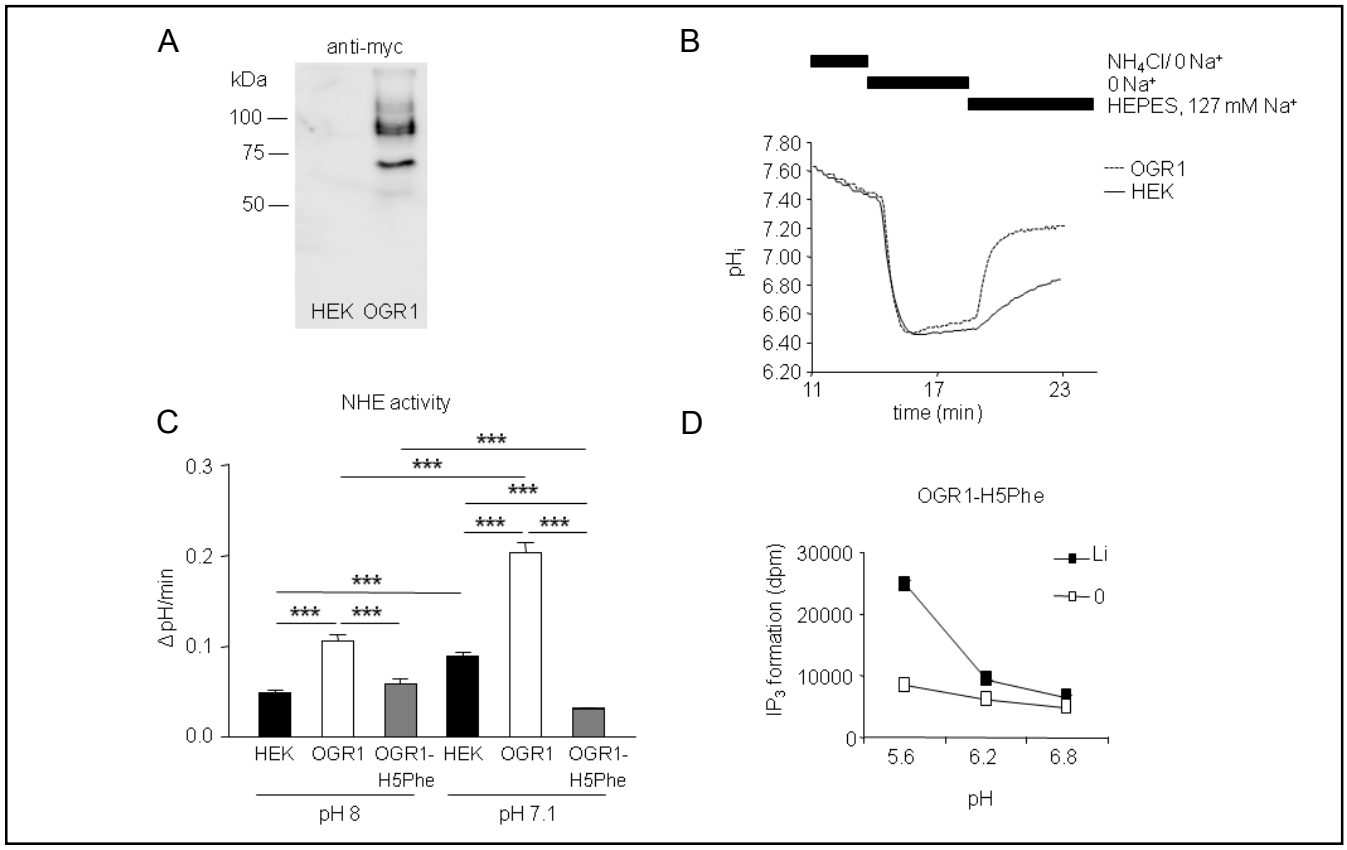

Fig. 1. pH-dependent stimulation of the Na^+/H^+ exchanger activity in OGR1 expressing cells. (A) Expression of myc-tagged human OGR1 was detected and confirmed in transfected cells but not in untransfected cells as two major bands around 65 and 85 kDa, respectively. (B) Original pH_i tracing of single representative HEK293 and HEK-OGR1 expressing cells. Bars indicate solutions present: removal of NH_4Cl from the bath causes a rapid intracellular acidification, in the absence of sodium no or only a slow realkalinization is observed, addition of sodium to the bath re-alkalinizes cells due to sodium/proton exchanger activity as described previously (24). The initial rate of alkalinization after addition of sodium was faster in HEK293B cells expressing OGR1. (C) Summary of NHE activities at pH 8 and pH 7.1 in HEK293, HEK293 cells transfected with OGR1 or the H5PHE OGR1 mutant. HEK293 cells untransfected (HEK), HEK293 cells stably transfected with human OGR1 (OGR1) or the OGR1 mutant where 5 histidine residues were mutated to phenylalanine (OGR1-H5Phe) were preincubated for 10 min in HEPES buffer at pH 8 or 7.1 before starting pH_i measurements. Each bar represents measurements from at least 3 different batches of cells, ***p <0.001. (D) IP_3 formation was measured in stably transfected HEK293 cells expressing the OGR1 mutant H5Phe in the absence (0) or presence of lithium (Li). OGR1-H5Phe expressing cells have a markedly reduced IP_3 formation at pH 6.8 where the wild type receptor is fully active (11).

differences in the initial experiments between two different clones (level of protein expression of OGR1 and effects in intracellular pH measurements), we continued the experiments in only one clone (clone C44). Successful expression of OGR1 was tested by western blotting (Fig. 1A), which demonstrated the presence of OGR1 in transfected cells. Two major bands were observed at approx. 70 kDa and 90 kDa.

To examine the effect of OGR1 activation on sodium/proton exchange (NHE) activity, we performed intracellular pH measurements with the pH_i-sensitive dye BCECF in the human renal cell line HEK293 at two different extracellular pH values. Cells were preincubated for 20 min in HEPES buffer at pH 8 to reduce basal OGR1 activity. The Na^+-dependent recovery rate indicating NHE activity was significantly increased in OGR1-transfected cells compared to nontransfected HEK293 cells at baseline pH 8 (0.11 ± 0.007 vs. 0.05 ± 0.002 units pH/ min) (Fig. 1C, Table 2). This difference could be due to residual stimulation of NHE activity by OGR1. Preincubation of cells for 20 min at pH 7.1 to stimulate OGR1 activity caused an even more pronounced stimulatory effect on NHE activity (0.20 ± 0.010 vs. 0.09 ± 0.003 units pH/ min) (Fig. 1B, C, Table 2).

In contrast, cells expressing the OGR1 mutant (5 extracellular histidine residues mutated to phenylalanine: OGR1-H5Phe) showed the same activity as nontransfected HEK293 cells at pH 8 (0.06 ± 0.006 vs.

Cell experiments	Na^+-independent pH_i recovery	No. of cells (tubule fragments)	Na^+-dependent pH_i recovery	No. of cells (tubule fragments)
HEK, pH 8	0.004 ± 0.001	100 (6)	0.05 ± 0.002	47 (3)
HEK-OGR1, pH 8	-0.007 ± 0.001$^{\dagger 2}$	119 (8)	0.11 ± 0.007$^{\dagger 2}$	115 (6)
HEK-OGR H5Phe, pH 8	0.009 ± 0.001$^{\ddagger \#2}$	74 (4)	0.06 ± 0.006$^{\ddagger 2}$	74 (4)
HEK, pH 8 + BAPTA	0.025 ± 0.001	74 (4)	0.07 ± 0.004	74(4)
HEK-OGR1, pH 8 + BAPTA	0.025 ± 0.010	68 (4)	0.03 ± 0.002†	68 (4)
HEK, pH 7.1	0.008 ± 0.001	165 (10)	0.09 ± 0.003	165 (10)
HEK-OGR1, pH 7.1	0.013 ± 0.001$^{\dagger 2}$	270 (16)	0.20 ± 0.010$^{\dagger 2}$	262 (16)
HEK-OGR1 H5Phe, pH 7.1	0.006 ± 0.001$^{\ddagger 2}$	90 (5)	0.03 ± 0.001$^{\ddagger \#2}$	90 (5)
HEK, pH 7.1 + $ZnCl_2$	0.008 ± 0.001	78 (4)	0.07 ± 0.002	78 (4)
HEK-OGR1, pH 7.1 + $ZnCl_2$	0.017 ± 0.006	106 (7)	0.14 ± 0.014$^{\S 1}$	80 (7)
HEK, pH 7.1 + $CuCl_2$	0.013 ± 0.002	75 (4)	0.06 ± 0.003	75 (4)
HEK-OGR1, pH 7.1 + $CuCl_2$	0.014 ± 0.001	70 (4)	0.12 ± 0.008$^{\S 2}$	74 (4)
HEK, pH 7.1 + psychosine	0.005 ± 0.001	95 (5)	0.08 ± 0.002	95 (5)
HEK-OGR1, pH 7.1 + psychosine	0.005 ± 0.001$^{\S 2}$	59 (3)	0.17 ± 0.009	59 (3)
HEK, pH 7.1 + chelerythrine	-0.007 ± 0.001	75 (4)	0.08 ± 0.005	75 (4)
HEK-OGR1, pH 7.1 + chelerythrine	-0.001 ± 0.0003	103 (6)	0.04 ± 0.002$^{\S 2}$	102 (6)
HEK, pH 7.1 + PD098059	0.003 ± 0.001	76 (5)	0.03 ± 0.006	79 (5)
HEK-OGR1, pH 7.1 + PD098059	0.002 ± 0.0004	49 (3)	0.11 ± 0.007$^{\S 2}$	49 (3)
HEK, pH 7.1 + BAPTA	0.001 ± 0.0003	36 (2)	0.07 ± 0.002	36 (2)
HEK-OGR, pH 7.1 + BAPTA	0.003 ± 0.001	48 (4)	0.03 ± 0.005†	48 (4)
Mouse experiments				
Ogr1$^{+/+}$ proximal tubule, pH 8	0.09 ± 0.002	101 (7)	0.26 ± 0.02	101 (7)
Ogr1$^{-/-}$ proximal tubule, pH 8	0.07 ± 0.003^{2}	80 (6)	0.22 ± 0.02	81 (6)
Ogr1$^{+/+}$ proximal tubule, pH 7.1	0.04 ± 0.0002$^{\&2}$	73 (6)	0.31 ± 0.02	73 (6)
Ogr1$^{-/-}$ proximal tubule, pH 7.1	0.05 ± 0.003$^{\&2\,1}$	90 (8)	0.36 ± 0.02$^{\&2}$	90 (8)

Table 2. Summary of intracellular pH (pH_i) measurements in cells (HEK293, HEK-OGR1 transfected and the HEK-OGR1-H5PHe mutant) and in proximal tubule fragments from wild type and OGR1 deficient mice. Data are presented as mean ± SEM. If not stated otherwise, substances were used at the following concentrations: $ZnCl_2$ 100 µM, $CuCl_2$10 µM; psychosine 10 µM; Chelerythrine 1 µM; PD098059 20 µM. n.d., not determined. †significantly different between HEK and HEK-OGR1at pH 8 or 7.1 , ‡significantly different between HEK-OGR1 and HEK-OGR1-H5Phe at pH 8 or 7.1, #significantly different between HEK and HEK-OGR1-H5Phe at pH 8 or 7.1, §significantly different between HEK-OGR1 pH 7.1 and HEK-OGR1 pH 7.1 plus different inhibitors, &significantly different between *Ogr1*$^{+/+}$ or *Ogr1*$^{-/-}$ from pH 8 to pH 7.1, significantly different between *Ogr1*$^{+/+}$ and *Ogr1*$^{-/-}$ at pH 8 or pH 7.1. [1]represents $p<0.01$, and [2]$p<0.001$.

0.05 ± 0.002 units pH/ min) that could not be stimulated by changing the pH to 7.1 (0.03 ± 0.001 units pH/ min) (Fig. 1C). Mutation of the 5 histidine residues reduced and left shifted the OGR1 dependent increase in intracellular IP_3 formation (Fig. 1D) as described previously [11]. These results demonstrate that overexpression of OGR1 by itself does not stimulate NHE activity but that its receptor activity is required. To determine the affected NHE isoform we used S3226 as a specific inhibitor of the NHE subtype 3 (NHE3) [25]. Addition of 100 nM S3226 resulted in a significant decrease of the NHE activity at pH 7.1 in OGR1 transfected cells suggesting NHE3 as the main type of NHE involved (0.20 ± 0.010 units pH/ min in the absence of S3226 vs. 0.05 ± 0.004 units pH/ min in the presence of S3226; data not shown).

pH-dependent changes of the H^+-ATPase activity in cells

In contrast to the NHE activity, the Na^+-independent pH_i recovery of OGR1 transfected cells was reduced at pH 8 compared to HEK control cells (-0.007 ± 0.0009 vs. 0.004 ± 0.0007 units pH/ min, respectively). This de facto acidification may reflect metabolic production of protons in the absence of any active proton extruding pathway. We have previously shown that the Na^+-independent pH_i-recovery rate is sensitive to the H^+-ATPase inhibitor bafilomycin and is thus due to the activity of V-type H^+-ATPases [24]. However, at pH 7.1 H^+-ATPase activity of OGR1 transfected cells was significantly stimulated versus control cells (0.013 ± 0.0007 vs. 0.008 ± 0.0009 units pH/ min, respectively). In contrast to the OGR1 transfected clone, OGR1 inactive mutant

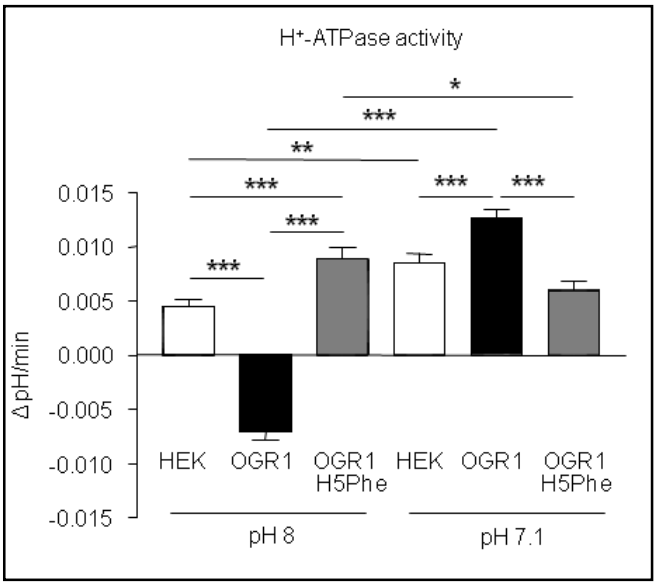

Fig. 2. OGR1 stimulates H^+-ATPase activity. The rate of Na^+-independent pH_i recovery was reduced at pH 8 and increased at pH 7.1 in OGR1 transfected cells. In contrast, OGR1-H5Phe cells demonstrated an increase at pH 8 and decreased activity at pH 7.1. Each bar summarizes data from at least 3 different batches of cells. *p <0.05, **p <0.01, ***p <0.001.

cells showed a higher H^+-ATPase activity at pH 8 and a reduction at pH 7.1 (0.009 ± 0.0010 vs. 0.006 ± 0.0009 units pH/ min, respectively) (Fig. 2, Table 2).

Inhibitory effect of $ZnCl_2$, $CuCl_2$, but not psychosine, on OGR1-dependent NHE activity

Micromolar concentrations of Zn^{2+} and Cu^{2+} ions inhibit OGR1-dependent IP_3 formation stimulated by lowering extracellular pH [11]. Moreover, psychosine has been implicated as an inhibitor of proton-dependent stimulation of OGR1 [26], even though the specificity of lipids in OGR1 stimulation or inhibition is controversial [12]. Thus, we tested whether or not $ZnCl_2$, $CuCl_2$, and psychosine have an effect on the OGR1-dependent stimulation of NHE and H^+-ATPase activity. $ZnCl_2$ and $CuCl_2$ at 10 µM significantly reduced the OGR1-dependent stimulation of the NHE activity at pH 7.1 (0.20 ± 0.010 vs. 0.14 ± 0.014 ($ZnCl_2$) and 0.12 ± 0.008 ($CuCl_2$) units pH/ min, respectively) (Fig. 3A, Table 2). Psychosine (10 µM) had no significant effect on NHE stimulation. Higher concentrations of psychosine (100 µM) often led to loss of BCECF from cells and detachment of cells suggesting cytotoxicity. In contrast, H^+-ATPase activity was significantly reduced by psychosine but not by $ZnCl_2$ and $CuCl_2$ (Fig. 3B, Table 2). Higher concentrations of these substances were also tested but resulted in unspecific effects (data not shown).

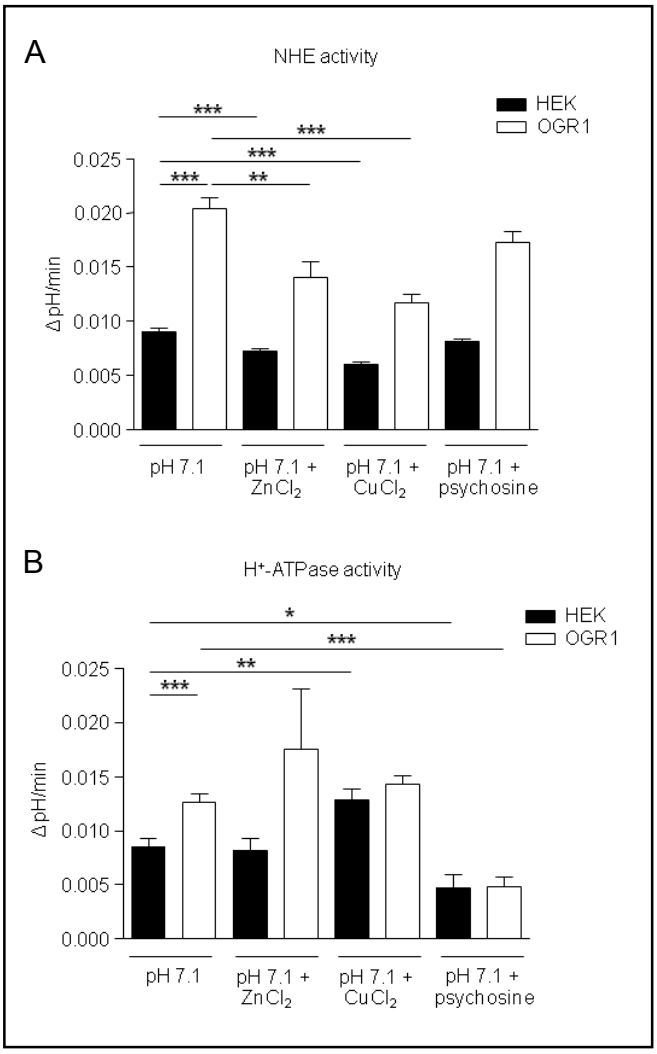

Fig. 3. $ZnCl_2$ and $CuCl_2$ reduce the OGR1 dependent stimulation of NHE and H^+-ATPase activity. $ZnCl_2$ (100 µM), $CuCl_2$ (10 µM), and psychosine (10 µM) were applied to all solutions. (A) $ZnCl_2$ and $CuCl_2$ reduced significantly the OGR1 dependent stimulation of NHE activity whereas psychosine had no effect. (B) Psychosine significantly reduced H^+-ATPase activity, but not by $ZnCl_2$ and $CuCl_2$. However, psychosine and $CuCl_2$ affected also basal H^+-ATPase activity. Each bar summarizes data from at least 3 different batches of cells. *p<0.05, **p<0.01, ***p<0.001.

Intracellular signaling mediating OGR1-dependent pH effects on NHE activity

OGR1 has been shown to couple to Gq proteins, phospholipase C, and to induce intracellular Ca^{2+} transients in transfected cells [11]. Similarly, signaling cascades activated by intracellular Ca^{2+} transients involving downstream signals such as PKC and the MAP-kinases ERK1/2 can stimulate NHE3 activity [27-29]. As previously reported [11], intracellular calcium concentration in OGR1-transfected cells increased when

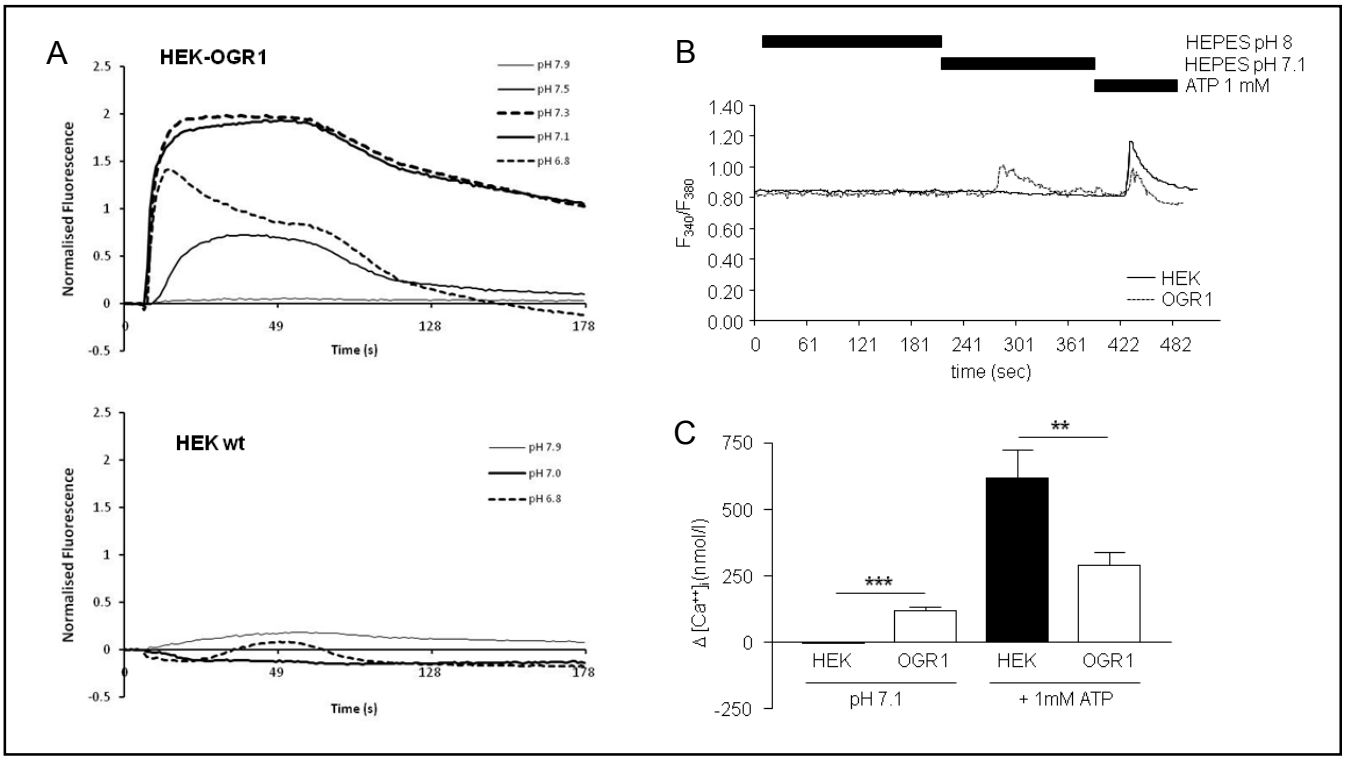

Fig. 4. pH-dependent increase of intracellular calcium in HEK293 and OGR1 expressing cells. (A) Untransfected or OGR1 transfected HEK293 cells were pre-incubated 60 min in HEPES buffer at pH 7.9 (during loading step) before starting calcium measurements. Extracellular pH was changed to values between 7.9 and 6.8. Intracellular calcium concentration in OGR1 transfected cells increased when cells were exposed to pH 7.5 and lower. (B, C) HEK293 or OGR1 transfected cells were pre-incubated 10 min in HEPES buffer at pH 8 before starting calcium measurements. Changing pH to 7.1 induced a significant increase in the intracellular calcium concentration in OGR1 transfected cells compared to HEK cells (shown as FURA-2 340/380 nm fluorescence ratio from a single OGR1 transfected cell compared to a HEK cell). ATP (1 mM) was used as a positive control. There is a 60 sec delay between switching solutions and reaching the chamber due to dead space in the perfusion system. Bar graph summarizing data from at least 3 different independent experiments from at least 3 different batches of cells. **p<0.01, ***p<0.001.

extracellular pH was switched from pH 7.9 to different pH values between 7.9 and pH 6.8 (Fig. 4A). In untransfected HEK293B cells, these changes in extracellular pH did not alter intracellular calcium concentrations significantly (Fig. 4A). In a second set of experiments, the calcium response was measured under the same conditions as for intracellular pH measurements. As expected, there was a significant increase of intracellular calcium concentration in OGR1-transfected cells compared to HEK control cells when extracellular pH was switched from pH 8 to pH 7.1 (-1.8 ± 0.75 vs. 117.3 ± 17.16 nM Ca^{2+}). ATP (1 mM) was subsequently applied to all cells to confirm viability (Fig. 4B, C). Using the intracellular calcium chelator BAPTA-AM confirmed the important role of calcium in the signaling cascade. Incubation with BAPTA-AM (100 μM) reduced basal NHE activity at pH 8 and prevented the increase in NHE activity when cells were incubated at pH 7.1. At pH 7.1, NHE activity was significantly reduced after addition of BAPTA-AM in OGR1 transfected cells when compared to untransfected cells (0.07 ± 0.004 vs. 0.03 ± 0.002) (Table 2). In contrast, H^+-ATPase activity was not changed between both cells.

Chelerythrine (1 μM), an inhibitor of PKC completely prevented the OGR1-dependent stimulation of NHE activity. In contrast, inhibition of ERK1/2 activation with PD 098059 (20 μM) decreased basal NHE activity but did not prevent the OGR1-dependent stimulation of NHE activity (Fig. 5, Table 2). Thus, OGR1 activation causes a transient increase of intracellular Ca^{2+} and stimulates NHE activity requiring intact PKC.

Modulation of Na^+/H^+ exchanger and H^+-ATPase activity in proximal tubules

We detected OGR1 mRNA in most segments of the mouse nephron by real-time PCR, including the proximal tubule and all subsegments of the collecting duct

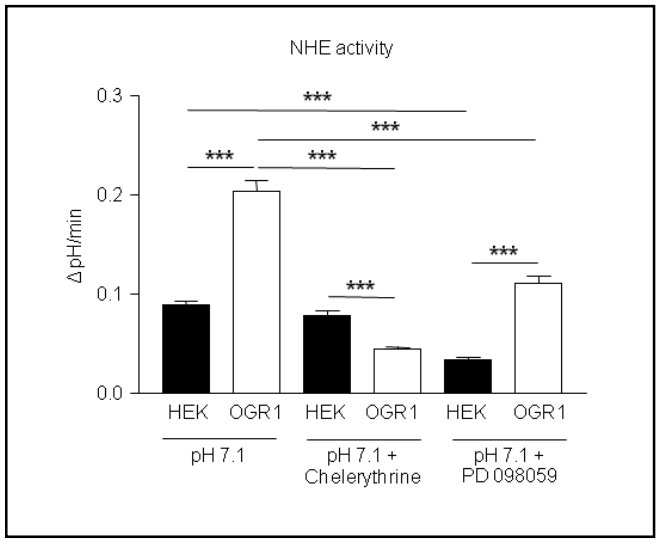

Fig. 5. OGR1-dependent stimulation of Na^+/H^+ exchanger activity requires PKC but not ERK1/2. The PKC inhibitor chelerythrine (1 μM) and the ERK1/2 inhibitor PD098059 (20 μM) were added to all solutions. Chelerythrine resulted in a significant decrease of the Na^+-dependent pHi recovery in OGR1 transfected cells but not in untransfected HEK293 cells at pH 7.1. Inhibition of the ERK1/2 pathway markedly reduced NHE activity in OGR1 transfected cells. However, the baseline NHE activity was also reduced by PD098059 and could be partly stimulated by OGR1. Each bar represents data from at least 3 different batches of cells. ***p<0.001.

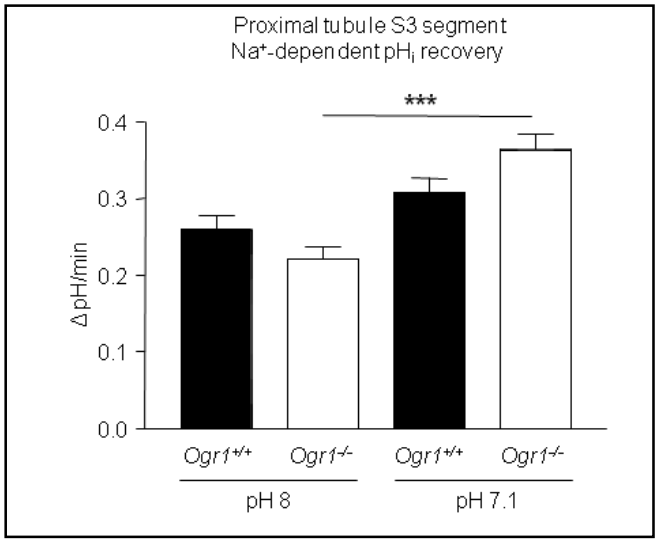

Fig. 6. pH-dependent changes of NHE and H^+-ATPase activity in proximal tubules of OGR1 deficient mice. In freshly isolated mouse proximal tubules Na^+/H^+ exchanger activity was measured as the rate of Na^+-dependent pH_i-recovery (in the nominal absence of bicarbonate) after preincubation of tubules at pH 8 or 7.1 for 10 min. NHE activity was stimulated in proximal tubules from *Ogr1*$^{-/-}$ but not from wild type mice. Each bar contains measurements from at least 3 different tubules from 3 different mice. **p<0.01, ***p<0.001.

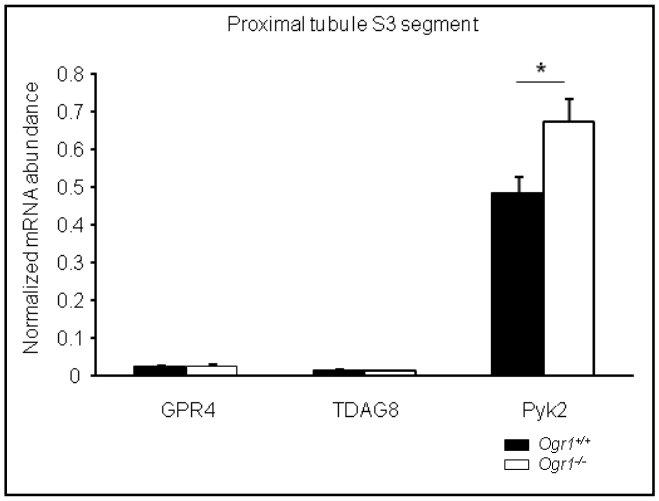

Fig. 7. mRNA expression of different pH-sensory molecules In isolated proximal tubule S3 segments from wildtype and OGR1 deficient mice. mRNA expression of GPR4, TDAG8 (GPR65), and Pyk2 were measured by real-time RT-PCR in hand-dissected isolated S3 segments of the proximal tubule from *Ogr1*$^{+/+}$ and *Ogr1*$^{-/-}$ mice. Data are given as mean ± SE; *n* = 4-5 animals/ group.

with highest abundance in the outer medullary collecting duct (data not shown). To assess the impact of OGR1-dependent effects of extracellular pH on NHE activity in native tissue, we isolated late proximal tubules from wild type and *Ogr1*$^{-/-}$ mouse kidneys and measured NHE activity at two different pH_o, pH 8 and pH 7.1. NHE activity in late proximal tubules from wild type mice tended to be higher when changing extracellular pH from pH 8 to 7.1. In contrast, in late proximal tubules of *Ogr1*$^{-/-}$ mice NHE activity was significantly stimulated at pH 7.1 compared to pH 8 (0.36 ± 0.02 vs. 0.22 ± 0.02 units pH/ min, respectively) (Fig. 6, Table 2). Thus, absence of OGR1 in the proximal tubule affects the response of NHE activity to changes in extracellular pH. Therefore, we tested by real-time RT-PCR if other potential pH-sensory molecules are regulated in a compensatory manner in *Ogr1*$^{-/-}$ mice (Fig. 7). In isolated S3 segments of the proximal tubule mRNA expression of the proton-activated receptors GPR4 and TDAG8 (GPR65) were not different between *Ogr1*$^{+/+}$ and *Ogr1*$^{-/-}$ mice. In contrast, Pyk2 mRNA expression was significantly increased in *Ogr1*$^{-/-}$ animals when compared to wild-type mice (0.67 ± 0.13 vs. 0.49 ± 0.09) (Fig. 7).

Discussion

We used two different approaches to examine the role of OGR1 in the context of the acute regulation of

acid-base transport proteins. First, we studied renal epithelial cells (HEK293B) that were stably transfected with active OGR1 and its less active mutant OGR-H5Phe. Second, we used native tissues from wild type and OGR1 deficient mice. Our novel findings are that OGR1 modulates the activity of two major plasma membrane proton transport systems and that OGR1 may be involved in the regulation of intra- and/or extracellular pH. We believe that our findings could be clinically relevant because they address general physiological mechanisms.

The kidneys eliminate about 70 mmoles acid daily from a typical Western diet. The kidneys make precise adjustments in acid excretion according to variations in intake by relying on acid-base transporters such as the sodium-proton exchanger 3 (NHE3), the major Na^+/H^+ antiporter isoform in the renal proximal tubule, and the vacuolar type H^+-ATPases (H^+-ATPases) on the plasma membrane of proximal tubules [2, 30-32]. NHE3 and H^+-ATPase are both tightly regulated by acid-base status and hormones, most notably endothelin, aldosterone and angiotensin II [14, 33-37]. NHE3 activity is not directly regulated by protons but rather by a signaling pathway including pH-sensing signaling molecules [27, 29]. Alternatively, a membrane-bound proton-sensing receptor may affect these intracellular signals, thereby coupling extracellular pH and activity of renal acid-base transport. Consistently, a role for another proton activated receptor, GPR4, in renal control of urinary acidification was suggested [38].

Eukaryotic cells regulate intracellular pH and thus must sense pH and activate signaling pathways responsible for the adaptive response such as proton or bicarbonate secretion [1-2]. The role of protons as signaling molecules has been previously discussed in various contexts and a number of proton-activated channels or receptors have been identified [4-10]. Ludwig et al showed that OGR1 acts as a proton-activated receptor via IP_3 formation and release of intracellular calcium transients [11]. OGR1 was initially identified in ovarian cancer cells [39]. The receptor was later claimed to be activated by the lipid messengers sphingosylphosphorylcholine (SPC) and lysophosphatidylcholine (LPC) [40]. Similarly, the closely related GPR4 receptor was also said to signal via SPC and LPC [41]. Substantial doubt has since been cast upon these reports [42, 43]. In OGR1-deficient mice, no differences in SPC and LPC-induced effects could be observed [13], which is in line with the notion that OGR1 is not a lipid receptor but rather may act as a receptor for protons *in vivo*.

We found that in HEK293B cells, OGR1 acted as a sensor of extracellular pH and stimulated sodium/proton exchange and H^+-ATPase activity. Incubation of cells at pH 7.1 led to more than half-maximal activation of the receptor [11] and robustly stimulated NHE activity in OGR1 expressing cells, but not in cells lacking OGR1 or expressing the H5Phe mutant. The mutant reaches the cell surface and is expressed in the cell membrane [11], displays activation as shown by IP_3 formation; however, only at much more acidic extracellular pH than the wild type receptor. The findings thus support the idea that not the presence of OGR1, but instead its behavior mediates most of the effect of extracellular pH on NHE activity.

OGR1 couples to G_q proteins, phospholipase C, and induces intracellular Ca^{2+} transients in transfected cells [11]. The signaling pathway of NHE3 stimulation by acid consists of signaling cascades that include intracellular Ca^{2+} transients, PKC, and MAP kinases including ERK1/2 [28, 29, 44]. In agreement with these data, we found intracellular Ca^{2+} transients in OGR1 transfected cells. Chelation of intracellular Ca^{2+} with BAPTA completely abolished the stimulatory effect of OGR1 suggesting that the observed Ca^{2+} transients may play an important role in the OGR1 dependent stimulation of NHE activity in these cells. Moreover, addition of chelerythrine, a PKC inhibitor, completely prevented the OGR1-dependent stimulation of NHE activity. Interestingly, inhibition of the MEK/ERK kinases with PD98059 did not prevent stimulation of NHE activity by OGR1 but reduced overall NHE activity. Thus, ERK1/2 may play a role for basal NHE activity but may not have a critical role in the stimulatory pathway activated by OGR1. Future studies need to address the mechanism by which OGR1 affects NHE3 activity.

OGR1 activation stimulated IP_3 formation, which was inhibited by micromolar concentrations of $ZnCl_2$ and $CuCl_2$, [11]. The role of the lipid messenger, psychosine, is rather controversial. Psychosine has been reported as a ligand for the related receptors TDAG8 [26] and GPR4 [41]. However, the GPR4 data have since been retracted [43]. In our study, $ZnCl_2$ and $CuCl_2$ reduced the OGR1-dependent stimulation of NHE activity while psychosine had no effect on basal NHE activity and on the stimulation by OGR1. Higher concentrations of psychosine could not be used since unspecific effects on BCECF loading and retention were observed. Thus, psychosine most likely has no effect on OGR1 activation. $ZnCl_2$ and $CuCl_2$ did not affect H^+-ATPase activity despite the stimulatory effect of OGR1 coexpression and activity. The concentrations of $ZnCl_2$ and $CuCl_2$ used here cause only

a partial inhibition of OGR1-dependent IP_3 formation [11]. We could not use higher concentrations since the compounds exerted unspecific effects on basal NHE and H^+-ATPase activity. Possibly, NHE activation by OGR1 is more sensitive to the inhibitory effects of zinc and copper than H^+-ATPase activity.

To confirm and extend our results obtained with HEK293 cells, we tested the pH-dependent regulation of NHE activity in isolated proximal tubules of wild-type and OGR1-deficient mice. Others and we have previously shown that NHE activity in mouse proximal tubule is mainly due to the NHE3 isoform [15, 28]. Basal NHE activity was similar in proximal tubules from wildtype and OGR1 deficient mice. Acute changes in the extracellular pH of proximal tubules did not affect NHE activity in wild-type mice while OGR1-deficient mice demonstrated a significant increase in NHE activity. These observations are in contrast to the experiments described in OGR1 transfected HEK 293 cells and suggest major differences in the pH-sensitivity of the cells and the native proximal tubule. We hypothesize that OGR1 is not the only pH-sensing mechanism in mouse proximal tubules. In fact, the presence of Pyk2, a tyrosine kinase sensitive to intracellular pH changes and capable of regulating NHE3 activity has been described [27]. Our qPCR results demonstrate an upregulation of Pyk2 in isolated proximal tubule cells from OGR1 deficient mice, whereas GPR4 and TDAG8 were not altered. Therefore, this state-of-affairs may indicate that loss of OGR1 can be compensated and that the effects of OGR1 on transporters depend on the cellular context or that antagonistic signals are present *in vivo*. Clearly, further studies are required to address the function and signaling pathway of OGR1 *in vivo* in more detail.

In summary, OGR1 regulates two major proton extruding transporters, NHE3 and H^+-ATPase. The acid-activated signaling pathway of OGR1 involves PKC activity in cells and a histidine residue cluster. In addition, OGR1 alters the pH-sensitive response of NHE and H^+-ATPase activity in proximal tubules. Our study is the first to describe the impact of OGR1 on major epithelial acid-base transport proteins.

Acknowledgements

The Swiss National Science foundation to C.A. Wagner (3100A0-122217) supported the study. Nilufar Mohebbi received a long-term research fellowship from ERA-EDTA. A ZIHP PhD student fellowship supported C. Benabbas. The authors thank Friedrich Luft for critically reading the manuscript and very valuable comments. The authors are not aware of interest conflicts.

References

1 Casey JR, Grinstein S, Orlowski J: Sensors and regulators of intracellular pH. Nat Rev Mol Cell Biol 2010;11:50-61.

2 Wagner CA, Finberg KE, Breton S, Marshansky V, Brown D, Geibel JP: Renal vacuolar H^+-ATPase. Physiol Rev 2004;84:1263-1314.

3 Halestrap AP, Meredith D: The SLC16 gene family-from monocarboxylate transporters (MCTs) to aromatic amino acid transporters and beyond. Pflugers Arch 2004;447:619-628.

4 Beg AA, Ernstrom GG, Nix P, Davis MW, Jorgensen EM: Protons act as a transmitter for muscle contraction in C. elegans. Cell 2008;132:149-160.

5 Pfeiffer J, Johnson D, Nehrke K: Oscillatory transepithelial H^+ flux regulates a rhythmic behavior in C. elegans. Curr Biol 2008;18:297-302.

6 Lingueglia E: Acid-sensing ion channels in sensory perception. J Biol Chem 2007;282:17325-17329.

7 Venkatachalam K, Montell C: TRP channels. Annu Rev Biochem 2007;76:387-417.

8 Quinn SJ, Bai M, Brown EM: pH sensing by the calcium-sensing receptor. J Biol Chem 2004;279:37241-37249.

9 Doroszewicz J, Waldegger P, Jeck N, Seyberth H, Waldegger S: pH dependence of extracellular calcium sensing receptor activity determined by a novel technique. Kidney Int 2005;67:187-192.

10 Adebanjo OA, Shankar VS, Pazianas M, Zaidi A, Simon B, Huang CL, Zaidi M: Modulation of the osteoclast Ca^{2+} receptor by extracellular protons: Possible linkage between Ca^{2+} sensing and extracellular acidification. Biochem Biophys Res Commun 1994;199:742-747.

11 Ludwig MG, Vanek M, Guerini D, Gasser JA, Jones CE, Junker U, Hofstetter H, Wolf RM, Seuwen K: Proton-sensing G-protein-coupled receptors. Nature 2003;425:93-98.

12 Seuwen K, Ludwig MG, Wolf RM: Receptors for protons or lipid messengers or both? J Recept Signal Transduct Res 2006;26:599-610.

13 Li H, Wang D, Singh LS, Berk M, Tan H, Zhao Z, Steinmetz R, Kirmani K, Wei G, Xu Y: Abnormalities in osteoclastogenesis and decreased tumorigenesis in mice deficient for ovarian cancer G protein-coupled receptor 1. PLoS One 2009;4:e5705.

14 Winter C, Schulz N, Giebisch G, Geibel J P, Wagner CA: Nongenomic stimulation of vacuolar H^+-ATPases in intercalated renal tubule cells by aldosterone. Proc Nat Acad Sci USA 2004;101:2636-2641.

15 Wagner CA, Lukewille U, Valles P, Breton S, Brown D, Giebisch GH, Geibel JP: A rapid enzymatic method for the isolation of defined kidney tubule fragments from mouse. Pflugers Arch 2003;446:623-632.

16 Biver S, Belge H, Bourgeois S, Van Vooren P, Nowik M, Scohy S, Houillier P, Szpirer J, Szpirer C, Wagner CA, Devuyst O, Marini AM: A role for rhesus factor Rhcg in renal ammonium excretion and male fertility. Nature 2008;456:339-343.

17 Roos A, Boron WF: Intracellular pH. Physiol Rev 1981;61:296-434.

18 Thomas JA, Buchsbaum RN, Zimniak A, Racker E: Intracellular pH measurements in Ehrlich ascites tumor cells utilizing spectroscopic probes generated in situ. Biochemistry 1979;18:2210-2218.

19 Grynkiewicz G, Poenie M, Tsien RY: A new generation of Ca^{2+} indicators with greatly improved fluorescence properties. J Biol Chem 1985;260:3440-3450.

20 Berridge MJ, Downes CP, Hanley MR: Lithium amplifies agonist-dependent phosphatidylinositol responses in brain and salivary glands. Biochem J 1982;206:587-595.

21 Berridge MJ, Irvine RF: Inositol phosphates and cell signalling. Nature 1989;341:197-205.

22 Xie B, Tassi E, Swift MR, McDonnell K, Bowden ET, Wang S, Ueda Y, Tomita Y, Riegel AT, Wellstein A: Identification of the fibroblast growth factor (FGF)-interacting domain in a secreted FGF-binding protein by phage display. J Biol Chem 2006;281:1137-1144.

23 Seuwen K, Lagarde A, Pouyssegur J: Deregulation of hamster fibroblast proliferation by mutated ras oncogenes is not mediated by constitutive activation of phosphoinositide-specific phospholipase C. EMBO J 1988;7:161-168.

24 Lang K, Wagner CA, Haddad G, Burnekova O, Geibel J: Intracellular pH activates membrane-bound Na^+/H^+ exchanger and vacuolar H^+-ATPase in human embryonic kidney (hek) cells. Cell Physiol Biochem 2003;13:257-262.

25 Schwark JR, Jansen HW, Lang HJ, Krick W, Burckhardt G, Hropot M: S3226, a novel inhibitor of Na^+/H^+ exchanger subtype 3 in various cell types. Pflugers Arch 1998;436:797-800.

26 Wang JQ, Kon J, Mogi C, Tobo M, Damirin A, Sato K, Komachi M, Malchinkhuu E, Murata N, Kimura T, Kuwabara A, Wakamatsu K, Koizumi H, Uede T, Tsujimoto G, Kurose H, Sato T, Harada A, Misawa N, Tomura H, Okajima F: TDAG8 is a proton-sensing and psychosine-sensitive G-protein-coupled receptor. J Biol Chem 2004;279:45626-45633.

27 Li S, Sato S, Yang X, Preisig PA, Alpern RJ: Pyk2 activation is integral to acid stimulation of sodium/hydrogen exchanger 3. J Clin Invest 2004;114:1782-1789.

28 Bobulescu IA, Moe OW: Luminal Na^+/H^+ exchange in the proximal tubule. Pflugers Arch 2009;458:5-21.

29 Tsuganezawa H, Sato S, Yamaji Y, Preisig PA, Moe OW, Alpern RJ: Role of c-src and ERK in acid-induced activation of NHE3. Kidney Int 2002;62:41-50.

30 Aronson PS, Nee J, Suhm MA: Modifier role of internal H^+ in activating the Na^+-H^+ exchanger in renal microvillus membrane vesicles. Nature 1982;299:161-163.

31 Wagner CA, Devuyst O, Bourgeois S, Mohebbi N: Regulated acid-base transport in the collecting duct. Pflugers Arch 2009;458:137-156.

32 Wagner CA, Devuyst O, Belge H, Bourgeois S, Houillier P: The rhesus protein Rhcg: A new perspective in ammonium transport and distal urinary acidification. Kidney Int 2011;79:154-161.

33 Moe OW: Acute regulation of proximal tubule apical membrane Na/H exchanger NHE-3: Role of phosphorylation, protein trafficking, and regulatory factors. J Am Soc Nephrol 1999;10:2412-2425.

34 Ambuhl PM, Amemiya M, Danczkay M, Lotscher M, Kaissling B, Moe OW, Preisig PA, Alpern RJ: Chronic metabolic acidosis increases NHE3 protein abundance in rat kidney. Am J Physiol 1996;271:F917-925.

35 Rothenberger F, Velic A, Stehberger PA, Kovacikova J, Wagner CA: Angiotensin II stimulates vacuolar H^+-ATPase activity in renal acid-secretory intercalated cells from the outer medullary collecting duct. J Am Soc Nephrol 2007;18:2085-2093.

36 Wu MS, Biemesderfer D, Giebisch G, Aronson PS: Role of NHE3 in mediating renal brush border Na^+-H^+ exchange. Adaptation to metabolic acidosis. J Biol Chem 1996;271:32749-32752.

37 Licht C, Laghmani K, Yanagisawa M, Preisig PA, Alpern RJ: An autocrine role for endothelin-1 in the regulation of proximal tubule NHE3. Kidney Int 2004;65:1320-1326.

38 Sun X, Yang LV, Tiegs BC, Arend LJ, McGraw DW, Penn RB, Petrovic S: Deletion of the pH sensor GPR4 decreases renal acid excretion. J Am Soc Nephrol 2010;21:1745-1755.

39 Xu Y, Casey G: Identification of human OGR1, a novel G protein-coupled receptor that maps to chromosome 14. Genomics 1996;35:397-402.

40 Xu Y, Zhu K, Hong G, Wu W, Baudhuin LM, Xiao Y, Damron DS: Sphingosylphosphorylcholine is a ligand for ovarian cancer G-protein-coupled receptor 1. Nat Cell Biol 2000;2:261-267.

41 Zhu K, Baudhuin LM, Hong G, Williams FS, Cristina KL, Kabarowski JH, Witte ON, Xu Y: Sphingosylphosphorylcholine and lysophosphatidylcholine are ligands for the G protein-coupled receptor GPR4. J Biol Chem 2001;276:41325-41335.

42 Xu Y, Zhu K, Hong G, Wu W, Baudhuin LM, Xiao Y, Damron DS: Retraction: Retraction. Sphingosylphosphorylcholine is a ligand for ovarian cancer G-protein-coupled receptor 1. Nat Cell Biol 2006;8:299.

43 Zhu K, Baudhuin LM, Hong G, Williams FS, Cristina KL, Kabarowski JHS, Witte ON, Xu Y: Retraction: Sphingosylphosphorylcholine and lysophosphatidylcholine are ligands for the G protein-coupled receptor GPR4. J Biol Chem 2005;280:43280.

44 Donowitz M, Mohan S, Zhu CX, Chen TE, Lin R, Cha B, Zachos NC, Murtazina R, Sarker R, Li X: NHE3 regulatory complexes. J Exp Biol 2009;212:1638-1646.